


Cite this: *RSC Adv.*, 2021, 11, 35383

Combination of pose and rank consensus in docking-based virtual screening: the best of both worlds†

Valeria Scardino,^{ab} Mariela Bollini^c and Claudio N. Cavasotto^{id}*^{bde}

The use of high-throughput docking (HTD) in the drug discovery pipeline is today widely established. In spite of methodological improvements in docking accuracy (pose prediction), scoring power, ranking power, and screening power in HTD remain challenging. In fact, pose prediction is of critical importance in view of the pose-dependent scoring process, since incorrect poses will necessarily decrease the ranking power of scoring functions. The combination of results from different docking programs (consensus scoring) has been shown to improve the performance of HTD. Moreover, it has been also shown that a pose consensus approach might also result in database enrichment. We present a new methodology named Pose/Ranking Consensus (PRC) that combines both pose and ranking consensus approaches, to overcome the limitations of each stand-alone strategy. This approach has been developed using four docking programs (ICM, rDock, Auto Dock 4, and PLANTS; the first one is commercial, the other three are free). We undertook a thorough analysis for the best way of combining pose and rank strategies, and applied the PRC to a wide range of 34 targets sampling different protein families and binding site properties. Our approach exhibits an improved systematic performance in terms of enrichment factor and hit rate with respect to either pose consensus or consensus ranking alone strategies at a lower computational cost, while always ensuring the recovery of a suitable number of ligands. An analysis using four free docking programs (replacing ICM by Auto Dock Vina) displayed comparable results.

Received 30th July 2021
Accepted 26th October 2021

DOI: 10.1039/d1ra05785e

rsc.li/rsc-advances

Introduction

The experimental evaluation of chemical libraries for activity against a target of pharmaceutical interest through high-throughput screening has been long used in the drug discovery pipeline; however, this is both a time and resource consuming technique.¹ Computational methods are today valuable and established tools in all drug discovery endeavors, saving time, resources, and costs.^{2–4}

Among *in silico* methods in drug discovery, molecular docking has been widely used during the last three decades.^{4–6}

In protein-molecule docking, the optimal position, orientation and conformation (pose) of the molecule within the binding site is assessed (“docking stage”), and an estimation of its binding energy calculated. High-throughput docking (HTD) allows the screening of large chemical libraries (from thousands to millions of molecules) to generate a hit-list enriched with potential binders, which will be then advanced for biochemical and biological evaluation. To be computationally efficient, HTD involves several approximations at different levels,⁷ and the binding free energy calculation is later replaced by a docking score, which is a measure of the probability that the molecule will bind to the target. Thus, the docking stage is followed in this case by the “scoring stage”.^{7,8}

In spite of its undoubted success, HTD is not without challenges, since its performance depends on the energy representation of the system, the degree of target flexibility,^{4,9–11} and the consideration of water molecules within the binding site.^{4,12,13} A recent extensive comparison of docking programs showed that, in agreement with earlier works,^{14,15} they perform better in terms of docking accuracy (docking stage) than in terms of scoring power, ranking power, and screening power (scoring stage).¹⁶ We would like to stress that pose prediction is nevertheless of the utmost importance in molecular docking, since incorrect poses will result in meaningless scores, which would

^aMeton AI, Inc., Wilmington, DE, 19801, USA

^bAustral Institute for Applied Artificial Intelligence, Universidad Austral, Pilar, Buenos Aires, Argentina

^cCentro de Investigaciones en BioNanociencias (CIBION), Consejo Nacional de Investigaciones Científicas y Técnicas (CONICET), Ciudad de Buenos Aires, Argentina

^dComputational Drug Design and Biomedical Informatics Laboratory, Instituto de Investigaciones en Medicina Traslacional (IIMT), Universidad Austral-CONICET, Pilar, Buenos Aires, Argentina

^eFacultad de Ciencias Biomédicas, and Facultad de Ingeniería, Universidad Austral, Pilar, Buenos Aires, Argentina. E-mail: CCavasotto@austral.edu.ar; cnc@cavasotto-lab.net

† Electronic supplementary information (ESI) available. See DOI: 10.1039/d1ra05785e



thus reduce the ranking capacity of scoring functions. The performance of HTD using different docking programs has been further evaluated on several systems,^{17–19} and many inconsistencies have been found, such as different performances across programs, also showing that the effectiveness of each scoring function is system dependent.^{18,20,21} Several efforts have been conducted to improve the reliability at the scoring stage, such as machine-learning-based scoring functions,^{22,23} and quantum mechanical-base scoring.^{24–29}

The combination of several docking programs (consensus scoring) has been shown to improve the performance of HTD.^{20,30–33} In 2013, Houston and Walkinshaw proposed for the first time a consensus docking procedure that used several docking programs to increase the reliability of the predicted poses.³³ Tuccinardi *et al.* later used ten docking protocols to evaluate pose consensus on database enrichment,³² and later extended their analysis to 36 benchmark targets of the DUD database.³¹ They obtained comparable results to Arciniegas and Lange's Docking Data Feature Analysis (DDFA), an approach for carrying out virtual screening analysis based on artificial neural networks which was among the best performing methods at the time.³⁴ To obtain good hit rates with their pose consensus strategy, molecules with at least seven matching poses between programs should be selected; in general, the best results were obtained with ten matching poses, which could represent a high computational cost. However, and more importantly, the number of ligands retrieved in most of those cases was very small, with the risk of being zero in some cases.³¹

It should be highlighted that in consensus scoring (or consensus ranking), for the sake of robustness, it would desirable that scores for a given molecule be combined only when the poses assessed by the different docking programs are similar. We thus present a new strategy that combines both pose and ranking consensus to overcome the limitations of each strategy when used in a stand-alone fashion, and thus increase the performance of HTD campaigns. This method, named Pose/Ranking Consensus (PRC) is consistent with theory in the sense that scores (or ranks) obtained with different programs are only combined when poses are coincident. Using four docking programs (ICM, rDock, Auto Dock 4, and PLANTS) we performed an exhaustive search to look for the best way of combining pose and rank requirements, and evaluated this new method over a wide range of targets that correspond to diverse protein families sampling different binding site properties. Our results show a consistent and improved performance compared to either pose consensus alone, or consensus scoring (ranking) alone strategies. This method is simple to use, simpler than machine learning consensus scoring methods, and displays an excellent performance also using free software programs.

Methods

Target systems preparation

The 34 targets listed in Table 1 were downloaded from the PDB. Water molecules and co-factors were deleted, except in the following cases (*cf.* Table S1†): (i) within 8 Å of the native ligand: Ca²⁺ in PA2GA and NRAM; Zn²⁺ in LKHA4 and ACE; Zn²⁺ and

Ca²⁺ in HDAC2; Zn²⁺ and Mg²⁺ in PDE5A; nicotinamide-adenine-dinucleotide phosphate (napd) in ALDR and DHI1; dihydro nicotinamide-adenine-dinucleotide phosphate (nadph) in DYR; flavine mononucleotide (fmn) in PYRD. In the case of water molecules, they were conserved within 4 Å of the native ligand in the following cases: for HSP90a, water molecules 2059, 2121, 2123, and 2236; FA7, 2440; FABP4, 303, 623, 634, 665; LKHA4, 1099, 1322; UROK, 6 and 61; PDE5A, 38 and 75 (in this case, a cluster of nine neighboring water molecules in contact with those two were also included). The structure of the Dopamine D₃ receptor was in the antagonist bound conformation, and that of β₂ adrenergic receptor was in the agonist bound conformation. In the case of the HMDH, XIAP, HIVRT and DHI1, two protomers (chains a and b) were included in the docking calculations.

Receptors were prepared with the ICM program³⁵ (version 3.8-7c; MolSoft, San Diego, CA 2020), in a similar fashion as in other works.²⁵ Missing residues and hydrogen atoms were added followed by a local energy minimization of the system. Polar and water hydrogens within the binding site were optimized using a Monte Carlo simulation in the torsional space. Glutamate and aspartate side chains were assigned a −1 charge, and lysine and arginine were assigned a +1 charge. Asparagine and glutamine were inspected for possible flipping and adjusted if necessary. Histidine tautomers were assigned according to their most favorable hydrogen bonding pattern.

Docking libraries

Docking chemical libraries were prepared for each target by merging a set of actives and their corresponding matching decoys according to similar physico-chemical properties and structural dissimilarity, which has been shown to ensure unbiased calculations in docking simulations.^{36,37} The number of actives, decoys and sources for each target are shown in Table S2.† For all molecules, chirality and protonation states were inherited from the corresponding original databases.

Docking calculations

For protein-molecule docking, five programs were used in total: ICM,³⁵ Auto Dock 4,³⁸ rDock,³⁹ PLANTS,⁴⁰ and Auto Dock Vina.⁴¹ The latter was used for the free software evaluation only, replacing ICM. These programs have different search algorithms and scoring functions as described in previous works.^{30,40} For all the HTD runs, the top scored conformation of each molecule was selected. The box center and dimensions were determined with ICM in such a way that all molecules in the chemical library would fit within the binding site, and then used for all programs. In rDock, the docking cavity was automatically built using the reference ligand method, which defines a docking volume of a given size around the binding mode of a known ligand.

Auto Dock Tools utilities³⁸ were used to prepare the input files for Auto Dock 4, where the Lamarckian genetic algorithm was used for a 20-run search for each compound using 1.75 million of energy evaluation. For PLANTS, the ChemPLP scoring function was used and speed 1 was set as search speed. For



Table 1 The 34 target proteins used in the molecular docking calculations

Receptor	Receptor code	Receptor	Receptor code
Thymidine kinase	KITH	Tyrosine-protein kinase ABL	ABL1
Phospholipase A2	PA2GA	Protein-tyrosine phosphatase 1B	PTN1
Coagulation factor VII	FA7	Inhibitor of apoptosis protein 3	XIAP
Hexokinase type IV	HXK4	Androgen receptor	ANDR
Cyclin-dependent kinase 2	CDK2	Renin	RENI
Cyclooxygenase-1	COX1	Glutamate receptor ionotropic, AMPA 2	GRIA2
Fatty acid-binding protein 4	FABP4	Aldose reductase	ALDR
Heat shock protein 90 alpha	HSP90a	Dihydrofolate reductase	DYR
Estrogen receptor alpha	ESR1	Dihydroorotate dehydrogenase	PYRD
Neuraminidase	NRAM	11-Beta-hydroxysteroid dehydrogenase 1	DHI1
β_2 Adrenergic receptor (agonist bound)	ADRB2	Angiotensin-converting enzyme	ACE
HMG-CoA reductase	HMDH	Progesterone receptor	PRGR
Dopamine D ₃ receptor (antagonist bound)	DRD3	Human immunodeficiency virus type 1 reverse transcriptase	HIVRT
Histone deacetylase 2	HDAC2	Purine nucleoside phosphorylases	PNPH
Leukocyte function associated antigen-1	LFA1	Protein kinase C beta	KPCB
Leukotriene A4 hydrolase	LKHA4	Insulin-like growth factor I receptor	IGF1R
Urokinase-type plasminogen activator	UROK	Phosphodiesterase 5A	PDE5A

rDock, a radius of $8.0 \text{ \AA} \pm 2.0 \text{ \AA}$ from a reference ligand binding mode was used to represent the cavity. For Vina, an exhaustiveness value of 8 was set. For ICM, a thoroughness of 2 was used for the search algorithm. All the other parameters for every software remained at their default values. On average, each program took between 13 and 130 seconds per core per molecule, with ICM being the fastest and Auto Dock 4 the slowest program.

Exponential consensus ranking

In the Exponential Consensus Ranking (ECR),³⁰ the consensus rank $ECR(i)$ for each molecule i is calculated as

$$ECR(i) = \frac{1}{\sigma} \sum_j \exp \left[-\frac{r_j(i)}{\sigma} \right] \quad (1)$$

where $r_j(i)$ is the rank of molecule i determined using the scoring function of program j , and σ is the expected value of the exponential distribution; the ECR was found to be quasi-independent on σ ,³⁰ and we used $\sigma = 10\%$ of the total number of molecules for each docking library. Since the ECR is based on rank rather than score, it is therefore independent on score units, scales and offsets.

Pose consensus approach

From the four HTD campaigns, four binding modes were obtained for each molecule in the database, which correspond to the 4 docking programs used. The RMSD among all combinations of these poses was calculated using the ICM software, which allowed for the calculation of the static deviation between molecules. Poses were considered to match if they were within 2.0 \AA RMSD. A molecule was considered to have three matching poses (MPs) if the three corresponding combinations of two poses matched. For four matching poses, the six corresponding combinations of two poses must be coincident.

Evaluation metrics

The enrichment factor (EF) is defined as

$$EF(x) = \frac{Hits_x}{N_x} \bigg/ \frac{Hits_{total}}{N_{total}} \quad (2)$$

where $Hits_x$ represents the number of actives present in a subset x of the docked library, N_x the number of molecules in subset x , $Hits_{total}$ is the total number of ligands within the entire chemical library, and N_{total} its total number of molecules. EF represents the probability of finding an actual ligand within subset x with respect to the probability of finding a ligand at random. Whenever a molecule was represented by multiple states regarding its protonation or chirality, a score was calculated for each state, and the lowest score among those was used to build the rank and thus to calculate the EF.

The hit rate (HR) was calculated as

$$HR(x) = \frac{Hits_x}{N_x} \quad (3)$$

and is a measure between 0 and 1 which represents the probability of finding an actual ligand within the subset x .

Results and discussion

For the HTD campaigns, we selected a benchmark set of 34 targets from diverse protein families, exhibiting different binding site properties, and including the presence of co-factors and water molecules (*cf.* Table S1†). The chemical libraries used are described in the Methods section (*cf.* Table S2†). Four docking programs were used, AutoDock 4, ICM, rDock and PLANTS, which have different search algorithms and scoring functions. Auto Dock Vina was also evaluated, but we selected only the best four performing programs to develop a method with the lowest computational cost for a future prospective





Next, we considered a combination of the three options A, B, and C, in the following fashion: if a molecule had a maximum of two MPs, the corresponding ranks obtained with those two programs should be within the top 5%; with a maximum of three MPs, those corresponding three ranks should be within the top 10%; with four MPs, the four ranks ought to be in the top 20%. While this strategy (named option D) showed a slightly less average EF than options B and C (20.0 vs. 25.7), there were no cases where actual ligands could not be found. Therefore, it was preferred over each individual option. We explored other combinations of ranking thresholds which are presented in Table S5,[†] but 5%, 10% and 20% for two, three and four MPs, respectively, was the best choice (similar results were also obtained with values of 5%, 10% and 25%).

Table 5 EF values and Active/Selected (A/S) molecule rate for option D (2 MPs – top 5%; 3 MPs – top 10%; 4 MPs – top 20%) and PRC (option D with an ECR top 1.5% threshold). For the PRC, the hit rate (HR = A/S) is also displayed for a clearer view of the results obtained

	Option D		PRC		
Receptor	A/S ^a	EF	A/S ^a	EF	HR
KITH	15/23	14.8	13/15	19.7	0.87
PA2GA	16/30	22.4	12/16	31.5	0.75
FA7	64/73	30.7	44/45	34.3	0.98
HXK4	15/50	11.6	9/23	15.2	0.39
CDK2	14/33	12.6	11/17	19.3	0.65
COX1	11/111	3.4	8/47	5.8	0.17
FABP4	20/37	27.6	20/25	40.9	0.80
HSP90a	11/39	11.4	8/21	15.4	0.38
ESR1	33/80	21.7	33/53	32.8	0.62
NRAM	14/29	14.0	9/19	13.8	0.47
ADRB2	53/101	21.1	35/60	23.4	0.58
HMDH	25/55	23.8	14/30	24.5	0.47
DRD3	7/77	3.6	6/48	5.0	0.13
HDAC2	23/68	19.2	21/43	27.7	0.49
LFA1	9/59	9.5	8/43	11.6	0.19
LKHA4	29/130	12.6	18/69	14.7	0.26
UROK	46/70	40.5	46/50	56.8	0.92
ABL1	36/125	17.3	33/75	26.4	0.44
PTN1	31/128	13.7	24/57	23.9	0.42
XIAP	4/8	26.2	3/6	26.2	0.5
ANDR	12/94	6.9	10/40	13.5	0.25
Renin	15/20	50.6	14/17	55.6	0.82
GRIA2	25/83	22.9	20/52	29.2	0.38
ALDR	55/135	23.5	51/81	36.3	0.63
DYR	34/112	22.8	24/70	25.8	0.34
PYRD	31/80	22.9	30/51	34.7	0.59
DHI1	23/245	5.6	21/136	9.2	0.15
ACE	27/86	19.2	22/59	22.8	0.37
PRGR	36/185	10.5	30/94	17.3	0.32
HIVRT	36/169	13.5	28/97	16.5	0.29
PNPH	29/87	22.8	26/51	34.9	0.51
KPCB	43/65	43.2	42/51	53.8	0.82
IGF1R	20/38	33.6	20/33	38.6	0.61
PDE5A	46/153	21.1	41/98	29.3	0.42
Average	27/85 ^b	20.0	22/50 ^b	26.1	0.50

^a Number of actives and selected molecules for each target. ^b Average (A)/average (S).

The best of both worlds: the PRC method

If the selected molecules were sorted by ECR, and only those in the top 1.5% were selected, an even better performance was obtained (Table 5). This approach was named the Pose/Ranking Consensus (PRC). We also evaluated threshold values between 0.5% and 2%, with 1.5% showing the best results.

Fig. 1 shows a schematic representation of this Pose/Ranking Consensus (PRC) pipeline. Starting from the binding poses and ranks obtained with the four docking programs, a pose/ranking filtering approach is carried out. For this, the maximum number of MPs (1–4) is assessed for each molecule, coupled with identifying those programs where the poses matched. Then, the ones with four MPs are identified and filtered according to the 20% rank threshold in the corresponding programs. The same is performed for three MPs (10% rank threshold), and two MPs (5% rank threshold). In parallel, the ECR method is calculated onto the whole database. The molecules that pass the pose/ranking filters are ordered by their corresponding ECR, previously calculated, and the ones in the top 1.5% are finally selected.

In Table 5, we show the performance of the PRC method in terms of EF and number of actual ligands (actives) retrieved for each target. EF values of option D selection strategy are also presented. The last column shows the hit rate (probability of finding an actual ligand within the selected pool of molecules) in the PRC selected compounds. It can be readily noticed from these results that both the pose/ranking filtering and ECR threshold requirements are important to achieve high EF values. The PRC showed the best performance in almost every target evaluated, with the exception of one case (NRAM) where the difference was minimal.

As can be seen from Table 5, our method results in very high enrichment values, with an appropriate number of ligands. The latter could be critical in a prospective scenario, where the number of actual ligands might be scarce. When viewed in terms of probability, an average hit rate of 50% is achieved on the subsets of molecules selected. The maximum value (98%)

was obtained for FA7 where 44 out of 45 selected molecules were ligands. DRD3 showed the lowest hit rate value (13%) and the lowest number of ligands retrieved (6). In 2016, Tuccinardi *et al.* achieved an average hit rate of 45% (vs. 50% with PRC), which they required to be at the level of the best performing methods.³¹ We note, however, that the results they report correspond to the maximum hit rate that can be obtained for each target, which depends on the number of MPs used, and therefore is not directly applicable in a prospective analysis.

This novel method achieves very high EF values, greatly surpassing previous pose consensus techniques and ranking consensus techniques, including the ECR, as it is shown in the next section. The results are especially higher for those targets that have a poor performance in the four docking programs (and ECR), reaching EFs of more than triple the values of EF1 ECR (see below and Table 6).

Performance of the PRC method compared to ECR in view of traditional metrics

To further evaluate the performance of the PRC method we compared the improvement against the ECR for every target. We chose the ECR as a comparison method since it presented a better performance than other traditional ranking consensus strategies (such as RbR or RbV).³⁰ Table 6 shows the EFs of the PRC method compared to those of ECR at 1% (EF1). We chose EF1 as it is a standard metric, widely used in virtual screening. The fold increase (the ratio between PRC EF and ECR EF1) is also presented for a clearer comparison of the results. It can be noticed that 27 out of 34 targets showed an increase in the EF. The remaining seven targets showed similar results in both strategies. On average, the PRC method had a 1.50-fold increase over ECR EF1. The improvements are especially noticeable in targets with low EF1 both on individual programs and on ECR; for example, EF values are increased by a factor of three in PRC for HSP90a, neuraminidase and renin. Regarding DRD3 (the worst performer in PRC), the four docking programs performed poorly on this target, and our method displayed a noticeably

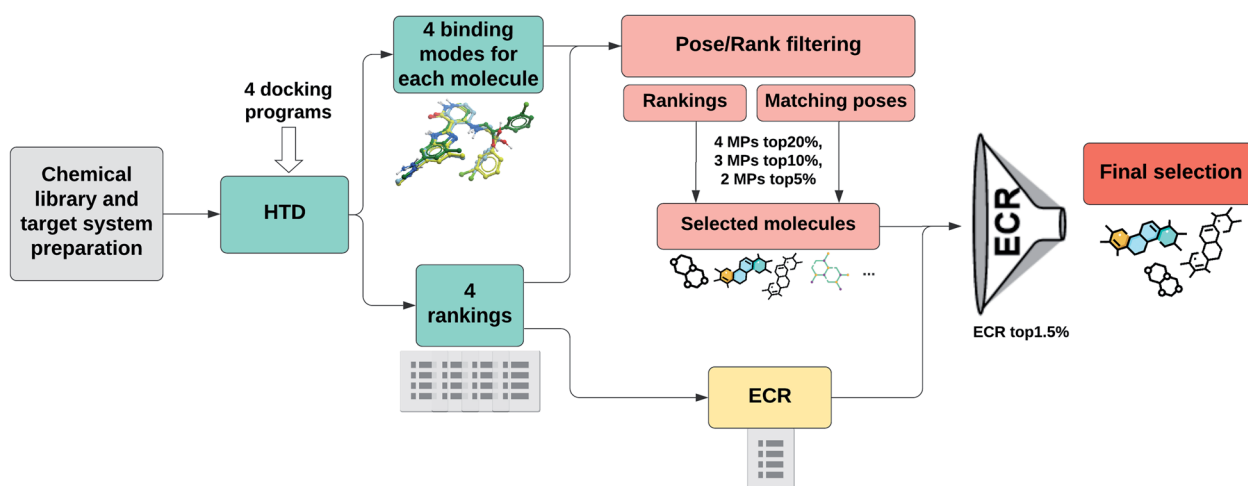


Fig. 1 PRC pipeline for high-throughput docking.



Table 6 Comparison of the EF at 1% (EF1) for ECR and the EF of PRC. The fold increase (PRC EF/ECR EF1) is also displayed in the last column

Receptor	ECR EF1	PRC EF	Fold increase
KITH	12.5	19.7	1.58
PA2GA	25.4	31.5	1.24
FA7	34.5	34.3	0.99
HXX4	5.5	15.2	2.76
CDK2	18.5	19.3	1.04
COX1	3.4	5.8	1.71
FABP4	40.5	40.9	1.01
HSP90a	4.9	15.4	3.14
ESR1	35.1	32.8	0.93
NRAM	4.5	13.8	3.07
ADRB2	24.5	23.4	0.96
HMDH	17.1	24.5	1.43
DRD3	3.2	5.0	1.56
HDAC2	13.6	27.7	2.04
LFA1	10.9	11.6	1.06
LKHA4	15.2	14.7	0.97
UROK	44.5	56.8	1.28
ABL1	25.3	26.4	1.04
PTN1	29.5	23.9	0.81
XIAP	20.2	26.2	1.30
ANDR	9.0	13.5	1.50
Renin	17.4	55.6	3.20
GRIA2	19.8	29.2	1.47
ALDR	33.5	36.3	1.08
DYR	26.1	25.8	0.99
PYRD	26.3	34.7	1.32
DHI1	8.8	9.2	1.05
ACE	14.3	22.8	1.59
PRGR	9.2	17.3	1.88
HIVRT	15.1	16.5	1.09
PNPH	37.1	34.9	0.94
KPCB	45.3	53.8	1.19
IGF1R	18.3	38.6	2.11
PDE5A	17.1	29.3	1.71
Average	20.3	26.1	1.50 ^a

^a Average of the fold increase values.

higher EF than ECR EF1. Table S6 in ESI† shows the same comparison (PRC vs. ECR) in terms of hit rates. On average, the ECR has a hit rate of 41% (vs. 50% in PRC).

We also analyzed for each target the ECR EF when selecting the same number of molecules from the top as those returned by the PRC. It should be noted that this is not a measure of practical value in prospective HTD, as this threshold is never known beforehand. However, the PRC in this case also surpassed the ECR, showing, on average, a 1.33-fold increase; moreover, our method showed an eight times higher EF in HXX4, and still showed 3-fold increase values in the worst performing targets.

Taking into account that the ECR already represents an improvement of the results over previous consensus strategies and to individual programs, these results show that the PRC method allows for significantly higher hit rates and EF values, with a minimal computational cost, and can therefore reach better results in future prospective HTD campaigns.

Performance of the PRC method using only free available docking programs

In some cases, it may happen that only free docking programs are available. Therefore, we present the results using only free and accessible programs. For this task, we replaced ICM with Auto Dock Vina, which was the other available software. Table 7 shows the results obtained after applying the PRC pipeline (Fig. 1) using Auto Dock 4, rDock, PLANTS and Auto Dock Vina for the HTD. For 2 MPs, we evaluated the possibility of excluding the combination of Auto Dock 4 and Auto Dock Vina, as we saw that there were many molecules that met this requirement. This exclusion allowed better results, and so it was maintained for the free programs procedure. The results of a solely pose consensus approach using free docking programs

Table 7 EF values and Active/Selected (A/S) molecule rate for option D (2 MPs – top 5%; 3 MPs – top 10%; 4 MPs – top 20%) and PRC (option D with an ECR top 1.5% threshold) using free docking programs. For the PRC, the hit rate (HR = A/S) is also displayed for a clearer view of the results obtained

Receptor	Option D		PRC		
	A/S ^a	EF	A/S ^a	EF	HR
KITH	3/17	4	3/9	7.6	0.33
PA2GA	11/16	28.9	10/13	32.4	0.77
FA7	27/40	23.7	22/29	26.6	0.76
HXX4	2/31	2.5	1/22	1.8	0.05
CDK2	17/34	14.9	12/22	16.3	0.55
COX1	11/236	1.6	5/91	1.9	0.05
FABP4	13/64	10.4	12/23	26.7	0.52
HSP90a	2/48	1.7	0/31	0	0
ESR1	36/159	11.9	31/80	20.4	0.39
NRAM	4/33	3.5	2/25	2.3	0.08
ADRB2	23/119	7.8	20/73	11.1	0.27
HMDH	16/41	20.4	7/21	17.5	0.33
DRD3	9/151	2.4	6/70	3.4	0.09
HDAC2	22/72	17.3	16/38	23.9	0.42
LFA1	10/86	7.3	9/53	10.6	0.17
LKHA4	46/181	14.3	31/74	23.6	0.42
UROK	46/89	31.9	43/62	42.8	0.69
ABL1	22/172	7.7	19/85	13.4	0.22
PTN1	28/80	19.8	23/43	30.3	0.53
XIAP	2/11	9.5	2/9	11.7	0.22
ANDR	14/164	4.6	13/97	7.3	0.13
Renin	9/18	33.7	9/13	46.7	0.69
GRIA2	25/95	19.9	16/51	23.8	0.31
ALDR	45/187	13.9	38/90	24.3	0.42
DYR	24/179	10.1	20/104	14.5	0.19
PYRD	28/88	18.8	24/50	28.3	0.48
DHI1	25/317	4.7	20/169	7.1	0.12
ACE	16/87	11.3	11/49	13.7	0.22
PRGR	36/313	6.2	21/149	7.6	0.14
HIVRT	32/269	6.7	14/150	5.3	0.09
PNPH	24/90	18.3	20/52	26.3	0.38
KPCB	41/92	29.1	39/56	45.5	0.70
IGF1R	20/61	20.9	20/42	30.4	0.48
PDE5A	44/210	14.7	39/140	19.5	0.28
Average	27/140 ^b	13.4	22/78 ^b	18.4	0.34

^a Number of actives and selected molecules for each target. ^b Average (A)/average (S).



are presented in Table S7.† Option D selection strategy is also displayed in Table 7 as a reference. The maximum hit rate (77%) was obtained for PA2GA where 10 out of 13 molecules selected were active. For HSP90a, all the individual programs performed poorly, and no actual ligands could be found. On average, a hit rate of 34% was obtained. It can be noted that the best results were also obtained when combining the pose/ranking filters with the ECR threshold (PRC). However, option D is shown as a good alternative for targets that do not perform well in none of the programs used, as it is the case of HXK4, HSP90a and NRAM.

In Table 8 we compare the results of the PRC and ECR for free docking programs. Better results were obtained in 28 of the 34 targets with an average 1.62-fold increase of the PRC method over the ECR EF1. Of the remaining six, ANDR is the one that shows the highest decrease. In this target, the docking programs did not perform well, with rDock showing zero EF1. For HSP90a, neither the ECR nor the PRC exhibited good

results. In option D it achieved a slightly better EF than the ECR EF1, and it may be a better selection strategy for cases where individual performances in terms of scoring are very poor. Regarding ESR1 and ABL1, while they still show acceptable EF values, they performed slightly worse than ECR. This was also the case for ESR1 with the previous procedure (Table 6). It should be noted, anyway, that the number of selected molecules for this target (80) is higher than 1% of its database (67).

A very noticeable improvement of PRC over ECR can be seen for KITH, HXK4, NRAM, HMDH, renin and ACE, where EF values of more than double the ECR EF1 were obtained. The average fold increase was even higher than in the previous case (1.62 vs. 1.50), therefore confirming the applicability of PRC method even when only free docking programs were available.

Conclusions and perspective

A new method combining both pose and ranking consensus (PRC) is presented and evaluated in 34 diverse protein targets, displaying an improved performance with respect to either pose consensus alone, or consensus scoring alone approaches. Our method is especially robust in the sense that scores (and ranks) are only combined when poses are coincident within a 2 Å threshold. In the PRC method we used four docking programs to build consensus strategies (ICM, rDock, Auto Dock 4, and PLANTS), and performed a comprehensive analysis of the optimal way of combining pose and rank requirements, which greatly improved the results compared to individual programs, and also to previous consensus strategies. It should be noted that high hit rates were obtained with low computational cost, yielding an appropriate number of ligands. It was observed that PRC greatly improves the results even when only free available docking programs are used (replacing ICM by Auto Dock Vina).

In spite of the obvious success, we would like to point out two facts related to this methodology: (i) it is still dependent on the performance of the individual programs on the target. If no program managed to perform well, the PRC method would still improve the results obtained, but in a limited way; (ii) option D (*cf.* Table 5) is a good alternative in a prospective case when it is suspected that a little number of actual ligands might be present in the query database, or when the target belongs to a family of proteins that does not usually perform well in HTD campaigns, since it will likely retrieve more ligands. While (i) is a common limitation to all consensus strategies, PRC shows itself as a promising tool to by-pass it. In a follow-up contribution, we will evaluate the dependence of the method on the relationship between the number of ligands and decoys in the database for each target.

Conflicts of interest

There are no conflicts to declare.

Acknowledgements

This work was supported by the National Agency for the Promotion of Science and Technology (ANPCyT) (PICT-2017-

Table 8 Comparison of the EF at 1% (EF1) for ECR and the EF of PRC using free docking programs. The fold increase (PRC EF/ECR EF1) is also displayed in the last column

Receptor	ECR EF1	PRC EF	Fold increase
KITH	2.3	7.6	3.22
PA2GA	16.7	32.4	1.94
FA7	24.1	26.6	1.1
HXK4	0.8	1.8	2.23
CDK2	12.8	16.3	1.27
COX1	1	1.9	1.95
FABP4	19.4	26.7	1.38
HSP90a	0	0	1
ESR1	23.9	20.4	0.85
NRAM	0.5	2.3	5.12
ADRB2	10.8	11.1	1.03
HMDH	7.6	17.5	2.30
DRD3	3.1	3.4	1.11
HDAC2	16.3	23.9	1.46
LFA1	12.3	10.6	0.86
LKHA4	18.2	23.6	1.30
UROK	30.9	42.8	1.39
ABL1	18.2	13.4	0.74
PTN1	33.4	30.3	0.91
XIAP	6.1	11.7	1.92
ANDR	10.5	7.3	0.70
Renin	12.5	46.7	3.74
GRIA2	14.7	23.8	1.62
ALDR	25.3	24.3	0.96
DYR	10.4	14.5	1.39
PYRD	20.0	28.3	1.42
DHI1	6.1	7.1	1.16
ACE	5.0	13.7	2.74
PRGR	4.1	7.6	1.85
HIVRT	5.3	5.3	1
PNPH	25.4	26.3	1.04
KPCB	37.9	45.5	1.20
IGF1R	17.6	30.4	1.73
PDE5A	12.9	19.5	1.51
Average	13.7	18.4	1.62 ^a

^a Average of the fold increase values.



3767). CNC thanks Molsoft LLC (San Diego, CA) for providing an academic license for the ICM program. The authors thank the Centro de Cálculo de Alto Desempeño (Universidad Nacional de Córdoba) for granting the use of their computational resources.

References

- 1 S. S. Phatak, C. C. Stephan and C. N. Cavasotto, *Expert Opin. Drug Discovery*, 2009, **4**, 947–959.
- 2 W. L. Jorgensen, *Acc. Chem. Res.*, 2009, **42**, 724–733.
- 3 G. Schneider, *Nat. Rev. Drug Discovery*, 2017, **17**, 97–113.
- 4 F. Spyraakis and C. N. Cavasotto, *Arch. Biochem. Biophys.*, 2015, **583**, 105–119.
- 5 A. Ciancetta and S. Moro, in *In Silico Drug Discovery and Design: Theory, Methods, Challenges, and Applications*, ed. C. N. Cavasotto, CRC Press, Taylor & Francis Group, Boca Raton, FL, 2015, ch. 7, pp. 189–213.
- 6 A. Sulimov, D. Kutov, I. Ilin, D. Zheltkov, E. Tyrtshnikov and V. Sulimov, *SAR QSAR Environ. Res.*, 2019, **30**, 733–749.
- 7 C. N. Cavasotto and A. J. Orry, *Curr. Top. Med. Chem.*, 2007, **7**, 1006–1014.
- 8 I. A. Guedes, F. S. S. Pereira and L. E. Dardenne, *Front. Pharmacol.*, 2018, **9**, 1089.
- 9 C. N. Cavasotto and N. Singh, *Curr. Comput.-Aided Drug Des.*, 2008, **4**, 221–234.
- 10 P. Cozzini, G. E. Kellogg, F. Spyraakis, D. J. Abraham, G. Costantino, A. Emerson, F. Fanelli, H. Gohlke, L. A. Kuhn, G. M. Morris, M. Orozco, T. A. Pertinhez, M. Rizzi and C. A. Sotriffer, *J. Med. Chem.*, 2008, **51**, 6237–6255.
- 11 C. N. Cavasotto, M. G. Aucar and N. S. Adler, *Int. J. Quantum Chem.*, 2019, **119**, e25678.
- 12 A. Amadasi, J. A. Surface, F. Spyraakis, P. Cozzini, A. Mozzarelli and G. E. Kellogg, *J. Med. Chem.*, 2008, **51**, 1063–1067.
- 13 P. Cozzini, M. Fornabaio, A. Mozzarelli, F. Spyraakis, G. E. Kellogg and D. J. Abraham, *Int. J. Quantum Chem.*, 2006, **106**, 647–651.
- 14 C. N. Cavasotto and R. A. Abagyan, *J. Mol. Biol.*, 2004, **337**, 209–225.
- 15 O. Slater and M. Kontoyianni, *Expert Opin. Drug Discovery*, 2019, **14**, 619–637.
- 16 M. Su, Q. Yang, Y. Du, G. Feng, Z. Liu, Y. Li and R. Wang, *J. Chem. Inf. Model.*, 2019, **59**, 895–913.
- 17 S. S. Çınaroğlu and E. Timuçin, *J. Chem. Inf. Model.*, 2019, **59**, 3846–3859.
- 18 Z. Wang, H. Sun, X. Yao, D. Li, L. Xu, Y. Li, S. Tian and T. Hou, *Phys. Chem. Chem. Phys.*, 2016, **18**, 12964–12975.
- 19 W. Xu, A. J. Lucke and D. P. Fairlie, *J. Mol. Graphics Modell.*, 2015, **57**, 76–88.
- 20 A. Kukol, *Eur. J. Med. Chem.*, 2011, **46**, 4661–4664.
- 21 J. B. Cross, D. C. Thompson, B. K. Rai, J. C. Baber, K. Y. Fan, Y. Hu and C. Humblet, *J. Chem. Inf. Model.*, 2009, **49**, 1455–1474.
- 22 P. J. Ballester, *Drug Discovery Today: Technol.*, 2019, **32–33**, 81–87.
- 23 J. C. Pereira, E. R. Caffarena and C. N. Dos Santos, *J. Chem. Inf. Model.*, 2016, **56**, 2495–2506.
- 24 M. G. Aucar and C. N. Cavasotto, *Methods Mol. Biol.*, 2020, **2114**, 269–284.
- 25 C. N. Cavasotto and M. G. Aucar, *Front. Chem.*, 2020, **8**, 246.
- 26 S. M. Eyrilmez, C. Kopruluoglu, J. Rezac and P. Hobza, *ChemPhysChem*, 2019, **20**, 2759–2766.
- 27 A. V. Sulimov, D. K. Kutov, I. S. Ilin and V. B. Sulimov, *Biomed. Khim.*, 2019, **65**, 80–85.
- 28 C. N. Cavasotto and J. I. Di Filippo, *Mol. Inf.*, 2021, **40**, e2000115.
- 29 C. N. Cavasotto, N. S. Adler and M. G. Aucar, *Front. Chem.*, 2018, **6**, 188.
- 30 K. Palacio-Rodriguez, I. Lans, C. N. Cavasotto and P. Cossio, *Sci. Rep.*, 2019, **9**, 5142.
- 31 G. Poli, A. Martinelli and T. Tuccinardi, *J. Enzyme Inhib. Med. Chem.*, 2016, **31**, 167–173.
- 32 T. Tuccinardi, G. Poli, V. Romboli, A. Giordano and A. Martinelli, *J. Chem. Inf. Model.*, 2014, **54**, 2980–2986.
- 33 D. R. Houston and M. D. Walkinshaw, *J. Chem. Inf. Model.*, 2013, **53**, 384–390.
- 34 M. Arciniega and O. F. Lange, *J. Chem. Inf. Model.*, 2014, **54**, 1401–1411.
- 35 R. Abagyan, M. Totrov and D. Kuznetsov, *J. Comput. Chem.*, 1994, **15**, 488–506.
- 36 E. A. Gatica and C. N. Cavasotto, *J. Chem. Inf. Model.*, 2012, **52**, 1–6.
- 37 N. Huang, B. K. Shoichet and J. J. Irwin, *J. Med. Chem.*, 2006, **49**, 6789–6801.
- 38 G. M. Morris, R. Huey, W. Lindstrom, M. F. Sanner, R. K. Belew, D. S. Goodsell and A. J. Olson, *J. Comput. Chem.*, 2009, **30**, 2785–2791.
- 39 S. Ruiz-Carmona, D. Alvarez-Garcia, N. Foloppe, A. B. Garmendia-Doval, S. Juhos, P. Schmidtke, X. Barril, R. E. Hubbard and S. D. Morley, *PLoS Comput. Biol.*, 2014, **10**, e1003571.
- 40 O. Korb, T. Stutzle and T. E. Exner, *J. Chem. Inf. Model.*, 2009, **49**, 84–96.
- 41 O. Trott and A. J. Olson, *J. Comput. Chem.*, 2010, **31**, 455–461.

